Progress In Electromagnetics Research Letters, Vol. 43, 55–63, 2013

A NOVEL DESIGN OF LOW PROFILE HIGHLY DIRECTIVE ANTENNA WITH PARTIALLY REFLECTING SURFACE SUPERSTRATE

Xiao-Jing Qi*, Yong-Chang Jiao, Gang Zhao, and Kai-Lun Liang

National Laboratory of Science and Technology on Antennas and Microwaves, Xidian University, Xi'an, Shaanxi 710071, China

Abstract—This paper presents a new design of high-gain low-profile resonant cavity antenna. A novel partially reflecting surface (PRS) is adopted as the superstrate with the characteristics of high-reflection magnitude and low-reflection phase that allows the reduction of cavity height to about $\lambda/8$ and the enhancement of the gain by 10.73 dB. Several significant parameters that characterize the PRS superstrate are investigated based on the unit cell simulation. The measured results show that this method is effective, and this structure can provide a high-gain at the operating frequency. The measured results agree reasonably well with the simulated ones.

1. INTRODUCTION

Over the last few years, more and more researchers have great interest in metamaterials owing to their unique properties [1–4]. Metamaterial is a composite material which does not exist in nature and is designed to mimic the specific characteristics, such as high-impedance planes (HIP) [5], electromagnetic bandgap structures (EBG) [6], artificial magnetic conductors [7] and so on. Metamaterial has been widely used and extended in wireless communications. One such application is a metamaterial based Fabry-Perot cavity which is composed of perfectly electrically conducting (PEC) ground and PRS to control the phase variation was used to realize a compact and steerable antenna with an improvement of gain about 1.7 dB [8]. In [9], the metamaterial with a couple of metal grids presenting a low phase value which contribute to enhancement of the gain of antenna by 2.3 dB and lead to the turn of

Received 9 August 2013, Accepted 12 September 2013, Scheduled 14 September 2013
* Corresponding author: Xiao-Jing Qi (xjqi_maple@163.com).

the size of the cavity in the lengthways direction. The author used EBG superstrates and metamaterial ground planes to realize $\lambda/6$ resonant cavities in [10]. AMC surfaces have also found many applications in the design of directive and compact cavity antennas [11]. AMC can be used as ground planes in order to reduce antenna size and improve the gain [12, 13]. But the improvement of the gain is limited. AMC can also be placed above an antenna to reduce the cavity height and enhance its directivity significantly by acting as a reflector. Greater achievements of thin sub-wavelength resonant cavity antennas [14] have been obtained [15–17].

In this paper, we present a high-gain low-profile resonant cavity antenna. A novel PRS superstrate is used as a cover of the antenna to improve the directivity; the negative reflection phase values of the PRS alter the resonance condition of the cavity and significantly reduce the antenna profile to less than $\lambda/8$. Considering suitable periodic boundary condition, the properties of the PRS are investigated through a parametric study. Finally, a high-gain low-profile resonant cavity antenna is designed, fabricated, and tested. Measured results are given to demonstrate the performance of the proposed antenna.

2. ANALYSIS

The resonant cavity antenna is formed by a simple radiating source backed with a PEC ground plane and a PRS superstrate placed at a distance h. The PEC and the PRS is assumed to be homogeneous surfaces in the analysis. We can use a simple geometrical optics model to describe the function of the antenna. The excitation source is placed inside the resonant cavity. Waves emerge from the source, most of them are reflected by the PRS and travel long paths, as a result of multiple reflections between the ground plane and the superstrate. Phase shifts are introduced by the path length, the reflection phases of the PEC ground plane and the superstrate. The waves leaking through the PRS have equal phase in the normal direction, and then a resonance is achieved. The resonance condition [18] is written as

$$\frac{2\pi}{\lambda}2h - \varphi_{PEC} - \varphi_{PRS} = 2N\pi \quad N = 0, \pm1, \pm2, \pm3, \ldots \tag{1}$$

where h is the cavity height that defines the antenna profile, λ the free-space wavelength, φ_{PEC} the reflection phase of the PEC ground plane, φ_{PRS} the reflection phase of the superstrate, and N an integer. Due to the unalterable reflection phase of the superstrate used in the conventional resonant cavity, the cavity height is fixed to $\lambda/2$. Therefore, a PRS with negative reflection phase values would result in the reduction of the cavity height. The above analysis thus predicts

that the antenna profile can be reduced by means of minimizing the total phase shift ($\varphi_{PEC} + \varphi_{PRS}$). Hence, the antenna profile is determined by

$$h = (\varphi_{PEC} + \varphi_{PRS})\frac{\lambda}{4\pi} + \frac{N\lambda}{2} \quad N = 0, \pm 1, \pm 2, \pm 3, \ldots \tag{2}$$

3. PRS SUPERSTRATE PERFORMANCES

In order to control both the magnitude and phase of the reflection coefficient for PRS superstrate, $N \times N$ square ring apertures (FSS structure) and square patches (uni-planar EBG structure) are patterned onto the top and bottom surfaces of superstrate respectively. The superstrate has a thickness of 1.5 mm and a relative dielectric constant of 2.65. The detailed structures on the top and bottom surfaces of the unit cell are shown in the inset of Figs. 1(a) and (b). The square ring aperture has a length of L and a width of W. The square patch has a length of La. The PRS is periodic structure, and the period P of the unit cell is 5 mm. We can analyze its characteristics with its unit cell by using the Ansoft's HFSS software.

Figs. 2(a), (b), (c) and (d) show the simulated magnitude and phase of the reflection coefficient for the PRS with square ring apertures of different length and width. The minimum value of the reflection magnitude decreases from 0.94 to 0.74, the resonance frequency decreases from 8.3 to 6.8 GHz, and the curve of the reflection phase gradually shifts to lower frequency, as L is increased from 3

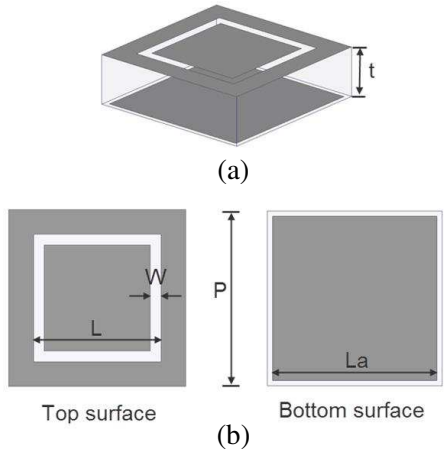

Figure 1. Geometry of the unit cell. (a) Schematic view of the unit cell, (b) unit cell patterns on the top and bottom surfaces.

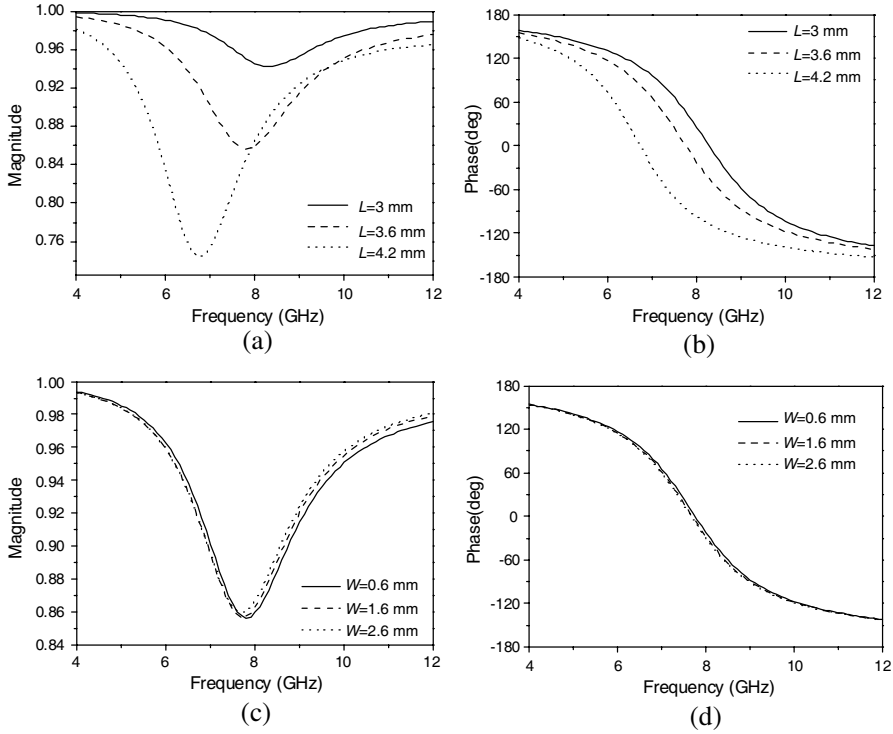

Figure 2. Simulated reflection coefficient of the PRS with various L and W ($La = 4.8\,\text{mm}$).

to 4.2 mm, respectively. As W is increased from 0.6 to 2.6 mm, the minimum value of the reflection magnitude and the reflection phase change slightly. It is found that the minimum reflection is mainly affected by L while very slightly affected by W.

The simulated reflection magnitude and phase of reflection coefficient versus La are shown in Figs. 3(a) and (b). As La is increased from 4.7 to 4.9 mm, the minimum value of the reflection magnitude increases from 0.86 to 0.87, the resonance frequency decreases from 8.3 to 7 GHz, and the curve of the reflection phase is shifted to lower frequency. From the results we find that, the resonance frequency is mainly affected by La, while the minimum value of the reflection magnitude have little displacement.

It is evident that the size of the square ring apertures has a great effect on reflection magnitude, while the size of square patches has a great influence on reflection phase. Thus the reflection magnitude and phase of the PRS at desired frequency can be tuned by adjusting the dimensions of L, W and La.

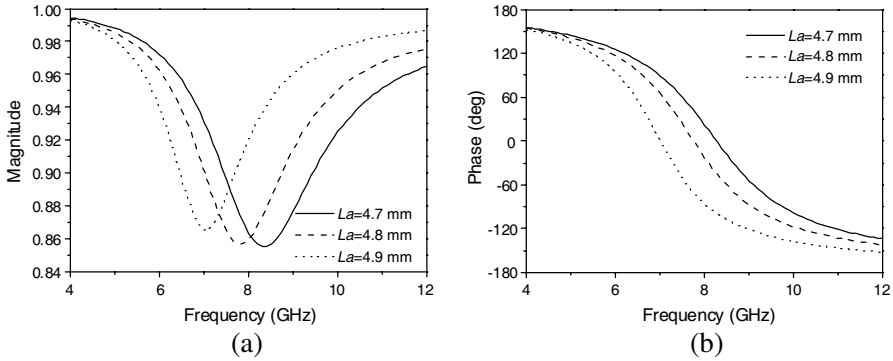

Figure 3. Simulated reflection coefficient of the PRS with various La ($L = 3.6\,\text{mm}$, $W = 0.6\,\text{mm}$).

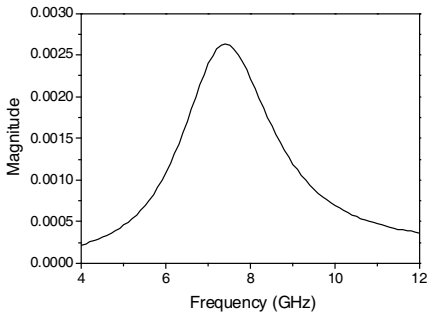

Figure 4. The ohmic losses coefficient of the PRS ($L = 3.6\,\text{mm}$, $W = 0.6\,\text{mm}$, $La = 4.8\,\text{mm}$).

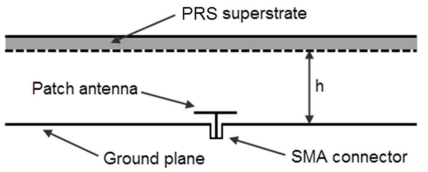

Figure 5. Geometry of the low-profile resonant cavity antenna.

4. ANTENNA DESIGN AND RESULTS

PRS and PEC ground plane with finite size are incorporated in a resonant cavity antenna configuration and simulated. Here we select the PRS surface with dimensions of $L = 3.6\,\text{mm}$, $W = 0.6\,\text{mm}$ and $La = 4.8\,\text{mm}$ as superstrate. The value of the reflection magnitude is close to 0.92 and the reflection phase is about -95° at the desired frequency (9.2 GHz), which ensures that high gain and low profile characteristics can be obtained. The ohmic losses coefficient of the PRS is shown in Fig. 4 and the value is about 0.00112 at 9.2 GHz. In this case, the thickness h was first predicted by using Eq. (2) at 9.2 GHz and then the optimal value was determined from experimental adjustment. The optimized thickness h is 4 mm, which corresponds to

(a) (b) (c)

Figure 6. Photographs of (a) PRS top surface, (b) PRS bottom surface, (c) whole structure.

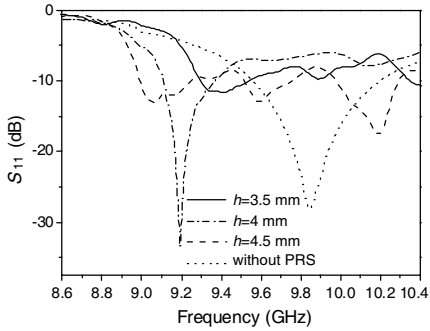

Figure 7. Measured reflection coefficient of the antenna with and without the PRS.

$\lambda/8$ at 9.2 GHz. Fig. 5 shows the proposed antenna configuration. The photographs of the PRS and the proposed antenna are shown in Fig. 6. The PRS has an area of $14 \times 14\,\text{cm}^2$ (about $4.3\lambda \times 4.3\lambda$ at 9.2 GHz) that covers 28×28 unit cells.

To obtain the better performance of the low-profile antenna, the height h is optimized in this paper and the result is shown in Fig. 7. The resonance frequency decreases from 9.42 to 9.07 GHz with the increase of h. When the PRS superstrate is placed above the patch antenna, the equivalent dielectric constant of the antenna is increased that makes the resonance frequency of the feed antenna decrease by 652 MHz. Both of the PRS and the patch antenna are working in a narrow band, so we can see from the result that the bandwidth of the cavity antenna is significantly reduced. The -10 dB return loss bandwidth is from 9.12 to 9.37 GHz and its relative bandwidth is

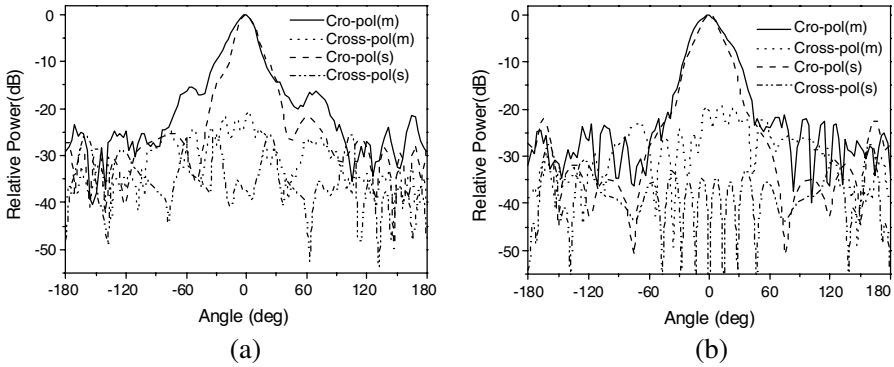

Figure 8. Measured and simulated radiation patterns of the resonant cavity antenna at 9.2 GHz. (a) E plane and (b) H plane.

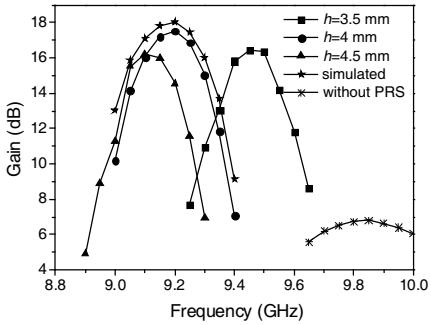

Figure 9. Gain along the Z axis for the antenna with and without the PRS.

2.83%. Figs. 8(a) and (b) show the measured and simulated radiation patterns of the antenna in E and H planes at the center frequency. In the measured result the half power beamwidth is 24° in E plane and 30° in H plane, and the front-to-back ratios of E and H planes are 29 dB and 34 dB, respectively. In the simulated result the half power beamwidth is 21° in E plane and 20° in H plane, and the front-to-back ratios of both E and H planes are 27 dB. The measured and simulated gain of the antenna is shown in Fig. 9. The peak gain of the antenna with and without the PRS is 17.52 dBi and 6.79 dBi respectively. With PRS superstrate the gain of the antenna is greatly improved by 10.73 dB. We can see from the result that the maximum gain can be obtained when the cavity height is adjusted to 4 mm. The bandwidth of the cavity antenna as defined from the -3 dB gain level is from 9.06 to 9.30 GHz or about 2.61%.

5. CONCLUSION

To summarize, a novel PRS surface with high-reflection magnitude and negative-reflection phase has been used as the superstrate of a resonant cavity antenna to achieve high gain and low profile performance. With the application of the PRS, the cavity height can be reduced to 4 mm, which is about one-eighth of the wavelength at the center frequency. Details of the antenna design are presented. The experimental results show that the proposed sub-wavelength resonant cavity antenna achieves a gain of 17.52 dBi at 9.2 GHz.

ACKNOWLEDGMENT

This work is supported by "the Fundamental Research Funds for the Central Universities".

REFERENCES

1. Attia, H., O. Siddiqui, L. Yousefi, and O. M. Ramahi, "Metamaterial for gain enhancement of printed antennas: Theory, measurements and optimization," *Saudi International Electronics, Communications and Photonics Conference (SIECPC)*, 1–6, Apr. 2011.
2. Enoch, S., G. Tayeb, P. Sabouroux, N. Guérin, and P. Vincent, "A metamaterial for directive emission," *Physical Review Letters*, Vol. 89, No. 21, 213902-1–213902-4, 2002.
3. Lagarkov, A. N., V. N. Kisel, and V. N. Semenenko, "Wide-angle absorption by the use of a metamaterial plate," *Progress In Electromagnetics Research Letters*, Vol. 1, 35–44, 2008.
4. Zhou, L., H. Li, Y. Qin, Z. Wei, and C. T. Chan, "Directive emissions from subwavelength metamaterial-based cavities," *Antenna Technology: Small Antennas and Novel Metamaterials*, Vol. 86, 101101-1–101101-3, 2005.
5. Sievenpiper, D., R. Broas, and E. Yablonovitch, "Antennas on high-impedance ground planes," *IEEE MTT-S Int. Microwave Symp. Digest*, Vol. 3, 1245–1248, 1999.
6. Ge, Y., K. P. Esselle, and Y. Hao, "Design of low-profile high-gain EBG resonator antennas using a genetic algorithm," *IEEE Antennas and Wireless Propagation Letters*, Vol. 6, 480–483, 2007.
7. Feresidis, A. P., G. Goussetis, S. Wang, and J. C. Vardaxoglou, "Artificial magnetic conductor surfaces and their application to low-profile high-gain planar antennas," *IEEE Transactions on Antennas and Propagation*, Vol. 53, No. 1, 209–215, 2005.

8. Boubakri, A. and J. Bel Hadj Tahar, "Steerable and compact antenna using a cavity-based metamaterial," *IEEE Mediterranean Microwave Symposium (MMS)*, 233–235, Nov. 2011.
9. Han, K., J. Fu, Q. Wu, and J. Hua, "The design and simulation of a metamaterial and subwavelength cavity-based antenna," *Cross Strait Quad-regional Radio Science and Wireless Technology Conference (CSQRWC)*, Vol. 1, 545–548, Jul. 2011.
10. Wang, S., A. P. Feresidis, G. Goussetis, and J. C. Vardaxoglou, "Low-profile resonant cavity antenna with Artificial magnetic conductor ground plane," *Antennas and Propagation Society International Symposium*, Vol. 4, 335–338, 2005.
11. Sohn, J. R., K. Y. Kim, H. S. Tae, and H. J. Lee, "Comparative study on various artificial magnetic conductors for low-profile antenna," *Progress In Electromagnetics Research*, Vol. 61, 27–37, 2006.
12. Abbasi, N. A. and R. J. Langley, "Multiband-integrated antenna/artificial magnetic conductor," *IET Microwaves, Antennas and Propagation*, Vol. 5, No. 6, 711–717, 2011.
13. Dewan, R., S. K. B. A. Rahim, S. F. Ausordin, and T. Purnamirza, "The improvement of array antenna performance with the implementation of an artificial magnetic conductor (AMC) ground plane and in-phase superstrate," *Progress In Electromagnetics Research*, Vol. 140, 147–167, 2013.
14. Kelly, J. R., T. Kokkinos, and A. P. Feresidis, "Analysis and design of sub-wavelength resonant cavity type 2-D leaky-wave antennas," *IEEE Trans. Antennas Propag.*, Vol. 56, No. 9, 2817–2825, Sep. 2008.
15. Zhao, G., Y. C. Jiao, F. Zhang, and F. S. Zhang, "Design of high-gain low-profile resonant cavity antenna using metamaterial superstrate," *Microwave and Optical Technology Letters*, Vol. 52, No. 8, 1855–1858, 2010.
16. Yang, F. H. and W. Tang, "A novel low-profile high-gain antenna based on artificial magnetic conductor for LTE applications," *2012 10th IEEE International Symposium on Antennas, Propagation and EM Theory (ISAPE)*, 171–174, 2012.
17. Ourir, A., A. de Lustrac, and J. M. Lourtioz, "All-metamaterial-based sub-wavelength cavities ($\lambda/60$) for ultrathin directive antennas," *Appl. Phys. Lett.*, Vol. 88, 084103-1–084103-3, 2006.
18. Lima, A. C. C. and E. A. Parker, "Fabry-Perot approach to the design of double layer FSS," *IEE Proceedings of Microwave, Antennas and Propagation*, Vol. 143, No. 2, 157–162, Apr. 1996.